ELSEVIER

NeuroImage

www.elsevier.com/locate/ynimg
NeuroImage 32 (2006) 1375 – 1384

Changes in the amplitude and timing of the hemodynamic response associated with prepulse inhibition of acoustic startle

Morris B. Goldman,[b,e,*] Linda Heidinger,[b] Kirti Kulkarni,[e,f] David C. Zhu,[h] Andrew Chien,[a] Donald G. McLaren,[g] Javaid Shah,[a] Charles E. Coffey Jr,[a] Sadia Sharif,[d] Elinor Chen,[c] Stephen J. Uftring,[c] Steven L. Small,[c,i] Ana Solodkin,[c,i] and Ramani S. Pilla[j]

[a]*Pritzker School of Medicine, University of Chicago, IL, USA*
[b]*Department of Psychiatry, University of Chicago, IL, USA*
[c]*The Brain Research Imaging Center, University of Chicago, IL, USA*
[d]*College of Arts and Sciences, University of Chicago, IL, USA*
[e]*Psychiatric Institute, University of Illinois at Chicago, IL, USA*
[f]*Department of Biomedical Engineering, University of Illinois at Chicago, IL, USA*
[g]*Departments of Anatomy and Neurobiology, Washington University School of Medicine, MO, USA*
[h]*Departments of Psychology and Radiology, and Cognitive Imaging Research Center, Michigan State University, MI, USA*
[i]*Department of Neurology, University of Chicago, IL, USA*
[j]*Departments of Statistics and Biology, Case Western Reserve University, OH, USA*

Received 22 January 2006; revised 26 April 2006; accepted 27 April 2006
Available online 14 July 2006

Disruption of the early stages of information processing in limbic brain circuits may underlie symptoms of severe neuropsychiatric disorders. Prepulse inhibition of acoustic startle (PPI) is diminished in many of these disorders and may reflect the disruption of this CNS function. PPI is associated with brain activity in many of the same regions in humans as it is in laboratory animals, suggesting that neuroimaging studies in humans may help localize deficits that can then be elucidated in animal models. In this article, we employed a rapid presentation event-related design during continuous EPI BOLD scanning to examine hemodynamic response functions (HRFs) associated with PPI. Fourteen healthy participants listened to 100 pulse alone and 100 prepulse combined with pulse (prepulse–pulse) trials. PPI is the normalized difference in the startle response to the two trial types. Following the prepulse–pulse trials, the amplitudes of the HRFs in auditory cortices and in the anterior insula were increased, while in the cerebellum, thalamus and anterior cingulate, they were decreased, relative to the pulse alone trials. In addition, the timing of the prepulse–pulse responses was delayed in the auditory cortices, anterior insula and cerebellum. Finally, PPI measured outside the scanner was predicted by the difference in BOLD responses between trial types in the anterior insula and in the cerebellum. The results suggest that prepulse inhibition, and by extension early stages of information processing, modulate both the amplitude as well as timing of neural activity.

Keywords: Prepulse inhibition; Event related; Auditory; Mental illness; Sensorimotor gating; Functional imaging

Introduction

Defects in the early stages of information processing have been associated with neuropsychiatric disorders for nearly a century (Bleuler, 1911; Meincke et al., 2004a; Hemsley, 2005). Recent advances in our understanding of the neural correlates of these processes in laboratory animals may help to characterize this circuitry in humans with the ultimate goal of defining and correcting the putative defects in patients. While several different paradigms probe early stages of information processing (Swerdlow et al., 2005), the paradigm most often linked to psychopathology (Wynn et al., 2005; Blumenthal, 1999), neuropsychiatric disorders (Dawson et al., 2000; Braff et al., 2001; Meincke et al., 2004b) and animal models (Weiss and Feldon, 2001; Swerdlow et al., 2001; Geyer et al., 2002; Van den Buuse et al., 2003) is the prepulse inhibition (PPI) of acoustic startle. PPI refers to the reduction (usually reported as a percentage) in the reflex motor response to a brief startling stimulus (pulse) when it is immediately preceded by a brief non-startling stimulus (prepulse). The prepulse is thought to trigger a neural cascade that promotes sensory integration of diverse stimuli (Fendt et al., 2001; Thorne et al., 2005; Diederich and Koch, 2005), and the reduced motor response to startle

* Corresponding author. Department of Psychiatry-MC3077, University of Chicago Medical Center, 5841 South Maryland, Chicago, IL 60637, USA. Fax: +1 708 383 6387.
E-mail address: m-goldman@uchicago.edu (M.B. Goldman).
Available online on ScienceDirect (www.sciencedirect.com).

1053-8119/$ - see front matter © 2006 Elsevier Inc. All rights reserved.
doi:10.1016/j.neuroimage.2006.04.228

provides a readout of the efficacy of this 'protective' function (Swerdlow et al., 2005; Rissling et al., 2005).

PPI of the acoustic startle response in the rat is localized to a circuit in the pons and midbrain that includes the inferior and superior colliculi, pedunculopontine tegmental and caudal pontine reticular nuclei (Fendt et al., 2001; Diederich and Koch, 2005). Activity in this circuit is influenced by and, in turn, influences activity in the cerebellum as well as in limbic structures (i.e., medial prefrontal, nucleus accumbens, amygdala, ventral palladium, thalamus) associated with sensory integration and neuropsychiatric disorders in humans (Fendt et al., 2001; Swerdlow et al., 2001). In humans, positron emission tomography (PET) and fMRI studies demonstrate that both acoustic (Pissiota et al., 2002) and tactile (Dimitrova et al., 2002; Maschke et al., 2003) startling pulses increase the neural activity in several of these structures (e.g., cerebellum, pons, hippocampus), while structural imaging studies in humans demonstrate a direct relationship between the gray matter volume in these structures and percent PPI (Kumari et al., 2005). Using fMRI, Hazlett et al. (2001) reported that acoustic prepulse combined with pulse (i.e., prepulse–pulse) responses were of greater amplitude in the thalamus, were of diminished amplitude in the medial frontal cortex and were of similar amplitude in the right anterior cingulate compared to the responses to pulse alone.

Three studies have also explored whether neural activity differs in schizophrenic patients and healthy controls. In a PET study, Hazlett et al. (1998) reported that prefrontal activation was greater in healthy participants than patients during a PPI study. However, the authors only performed a single scan and thus could not distinguish whether differences within or between groups were attributable to responses to pulse stimuli, prepulse stimuli or other factors. Kumari et al. (2003) assessed the fMRI responses to pulse alone as well as to prepulse–pulse blocks using tactile (air puff to the neck) prepulses and pulses. Activated regions included those previously identified by Hazlett et al. (1998, 2001), as well as several other regions associated with prepulse inhibition in animals, and neuropsychiatric disease in humans. Responses to pulse alone blocks were similar in patients and healthy participants. Healthy participants' prepulse–pulse responses were increased in fourteen brain areas (e.g., thalamus, hippocampus, nucleus accumbens, supramarginal gyrus, inferior parietal lobe) and decreased in cerebellum, cuneus and middle occipital lobe relative to their pulse alone responses, whereas patients showed greater prepulse–pulse responses in eight areas (e.g., middle frontal gyrus, sensory motor cortices, inferior parietal lobe) and decreased responses in posterior cingulate, medial frontal gyrus and superior temporal gyrus relative to their pulse alone responses. These differences between the two trial types were greater in healthy controls than patients in all regions where healthy controls' responses differed between the two trial types except the hippocampus, whereas the difference between trial types was greater in the patients than controls in sensory motor cortices and superior temporal gyrus. In addition, percent PPI measured outside the scanner correlated with the magnitude of prepulse–pulse responses in the thalamus, ventral striatum and inferior parietal lobe across all subjects which further links these structures to PPI. A recent study extended these findings by assessing the effects of nicotine treatment on BOLD activity, while patients and controls underwent blocks of tactile prepulse–pulse and pulse alone trials (Postma et al., 2006). Nicotine enhances PPI in humans and animals, and several lines of evidence suggest that it facilitates sensory integration (Kumari and Postma, 2005). The authors found that nicotine enhanced BOLD activity in many of the same regions associated with greater prepulse–pulse activity in their previous study, including the striatum, thalamus, hippocampus, insula and anterior cingulate. Furthermore, the change in left hippocampal activity predicted the change in prepulse inhibition associated with nicotine treatment in an accompanying study conducted outside of the scanner. Finally, the BOLD response to nicotine was greater in patients than controls in both the thalamus and hippocampus.

In summary, previous imaging studies in humans indicate that neural activity associated with PPI occurs in the same regions that modulate PPI in animal models and that activity differs from controls in persons with schizophrenia particularly in brain regions implicated in neuropsychiatric illness. Furthermore, while the increase in BOLD activity associated with prepulse–pulse (versus pulse alone) trials was generally greater in controls than patients, the improvement in PPI due to nicotine was associated with greater BOLD increases in thalamus and hippocampus in the patients, consistent with the concept that basal cholinergic defects contribute to impaired sensory integration in schizophrenia. Here, we attempt to complement these previous efforts by imaging prepulse inhibition with a rapid presentation event-related experimental design. This design more closely resembles certain characteristics of the standard PPI protocol (i.e., event-related design consisting of randomly presented and spaced acoustic trials over a constant background) (Burock et al., 1998). Furthermore, this design enables a more sensitive examination of the underlying hemodynamic response function associated with each trial type (HRF), which may further clarify the significance of the findings. For instance, alterations in sensory processing may manifest as shifts in timing without otherwise altering the shape of the HRF (Henson et al., 2002), and these shifts may differ between patients and controls (Ford et al., 2005).

Methods

Subjects

Forty-one healthy first and second year graduate students (26 male, age range: 22–30 years) were recruited for the study. Participants were all moderately to strongly right handed based on a modified Edinburgh Handedness Inventory (Oldfield, 1971), free from personal as well as family history of psychiatric disorders and without history of any other neurological injury/disease. All detected 40 dB tones in the ranges of 250–6000 Hz. Normal brain anatomy was confirmed in the fifteen participants who underwent the fMRI portion of the study. All were paid for their time and provided informed consent following guidelines approved by the Institutional Review Board of the University of Chicago.

Simulated scanner study

Participants underwent a five-minute mock scanner study in which they heard 12 pulse alone trials (40 ms of 107 dB of white noise) and 12 prepulse–pulse trials (20 ms of 88 dB of white noise followed 120 ms later by a pulse trial (trial length of 180 ms)) presented in a random order with a mean interstimulus interval

(ISI) of 12 s (range 8 to 16 s). Scanner noise was reproduced by recording an echo-planar imaging sequence with both a Shure MS57 and the scanner microphone. The sound intensity in the mock scanner was adjusted to that measured at the opening of the actual scanner (115 dB: A Weighting, Radio Shack Meter 33-2055). Stimuli were generated with a Human Startle Response Monitoring System (SRLAB, San Diego Instruments, San Diego, CA) amplified by a Sony amplifier (Model STR-DE 185), modulated by an Audiosource graphics equalizer (Model EQ 100) and delivered through custom-designed piezoelectric speakers into air conduction headphones fitted with foam ear tips (NRH101, Scan Sound Inc. Coral Springs, FL). Headphone padding attenuated scanner noise by approximately 40 dB. Electromyographic (EMG) activity of the *orbicularis oculi* muscle of the right eye was recorded with Ag/AgCl electrodes in 250 one-millisecond epochs starting at the onset of each trial. Summation of the epochs into a muscle contraction wave, calculation of peak EMG activity and lastly percent PPI was carried out using standard parameters of the SRLAB (Braff et al., 1992).

Stimulus presentation during fMRI study

After 1 to 4 weeks, fifteen participants who exhibited the greatest PPI in the mock scanner underwent an fMRI study. Participants heard 100 pulse and 100 prepulse–pulse trials presented pseudorandomly in an event-related design. The hardware, trial stimuli and jittered ISI were otherwise identical to the simulated scanner study. Trial onset coincided with the beginning of a repetition time (TR) during functional data acquisition, and the startling pulses always occurred 140 ms after the beginning of a TR. Participants were instructed to stay awake and keep their eyes open.

fMRI data acquisition

Imaging was carried out in the Brain Research Imaging Center at the University of Chicago on a 3-T Signa scanner (GE Medical System, Milwaukee, WI) fitted with a standard GE head coil. Images were first acquired for the purpose of localization; next, first and higher-order shimming procedures were carried out to improve magnetic field homogeneity (Kim et al., 2002). Twenty-five contiguous 3.6-mm-thick slices, from the anterior tip of the genu of the corpus callosum to the posterior extent of the body of the corpus callosum, were collected in each TR. EPI BOLD coronal functional images (T_2*-weighted, 2000 ms TR, 26 ms time of echo (TE), 77° flip angle, fat saturation, 23 cm field of view) were acquired in an interleaved manner. There were four functional runs (50 trials per run) resulting in 1200 total volumes of images, with 3 min of rest between the first and second, as well as the third and fourth functional runs. Between the second and third runs, we obtained high-resolution volumetric T_1-weighted spoiled gradient-recalled images with cerebrospinal fluid suppressed. The images consisted of 124 1.5-mm-thick sagittal slices and 24 cm FOV. These images were used to identify anatomical locations and boundaries. Subjects were in the scanner for approximately 75 min.

fMRI data analysis

fMRI data pre-processing and initial data analysis were conducted with Analysis of Functional NeuroImages (AFNI) software using standard analytic approaches (Cox, 1996). Using the last image of the 2nd run as the reference, motion correction was applied in the three rotational and three translational directions, while also assessing to assure that movement was sub-voxel within runs. We also used the estimated amount of motion in the data analysis. Additional steps were taken to address movement-induced artifacts in each subject by: (1) comparing the absolute movement (i.e., $(x^2 + y^2 + z^2)^{1/2}$) in adjacent TRs which contained pulse trials, prepulse–pulse trials or neither trial type by analysis of variance (ANOVA); and (2) calculating the number of voxels with signal artifact during each run, while attempting to correct deviations. A single resampling of functional images using cubic spline interpolation compensated for asynchronous slice acquisition.

Individual subject's functional data were spatially smoothed using a Gaussian filter with 7.2 mm full width half maximum for all analyses except that used to define the False Discovery Rate (see below). Voxel-wise estimates of a 12-second BOLD response (coefficients) and associated statistics (F statistic) for each trial type were obtained through multiple linear regression on the smoothed functional data with the 3dDeconvolve software in AFNI (Ward, 2002). Thirty-two regressors were included in the model for this analysis: (a) the estimations of the three rotational and three translational corrections for motion (6 regressor variables); (b) a constant, linear and quadratic trend for the baseline BOLD signal for each of the four runs (12 regressor variables); (c) and seven regressor variables for each trial type representing the sampling points at trial onset as well as the subsequent 6 TRs (14 regressor variables). From this analysis, we obtained estimates for the regression coefficients for the seven sampling time points following each trial type for each voxel in each subject.

To facilitate comparison with data obtained by others (Kumari et al., 2003) and to identify candidate regions for the ROI analysis described below, a group analysis was next performed after first transforming each participant's data to Talairach space. In order to evaluate trial type differences, we fit a voxel-wise mixed-effects ANOVA model to obtain F statistics for the mean of the 3rd, 4th and 5th regression coefficients (i.e., covering the time period of the expected peak of the BOLD response) for each trial type (Neter et al., 1996). Significant regions of activity associated with each trial type and the difference between them were identified after correction for multiple comparisons which utilized a combination of voxel and cluster size thresholding (Fig. 1) (Forman et al., 1995).

Subsequently, a region of interest analysis (ROI) was performed to more completely characterize the underlying HRFs. Candidate regions were selected based on examination of the group data described above if there was a significant activity with either trial type (i.e., Fig. 1) or possible differences between trial types. ROIs were then selected based on examination of individual's data if there was significant BOLD activity (uncorrected threshold P value $<10^{-4}$) associated with either trial type in more than half the subjects in the candidate region. ROIs were then traced on each subject's anatomical scan using boundaries provided by an experienced neuroanatomist (AS) (Fig. 2). In order to restrict our characterization of the HRFs to active voxels within each ROI, we utilized the False Discovery Rate (defined as the proportion (q) of false positives relative to the number of detections; Genovese et al., 2002). We chose a q value of 0.2 to take into account the small effect sizes (Genovese et al., 2002). All seven regression

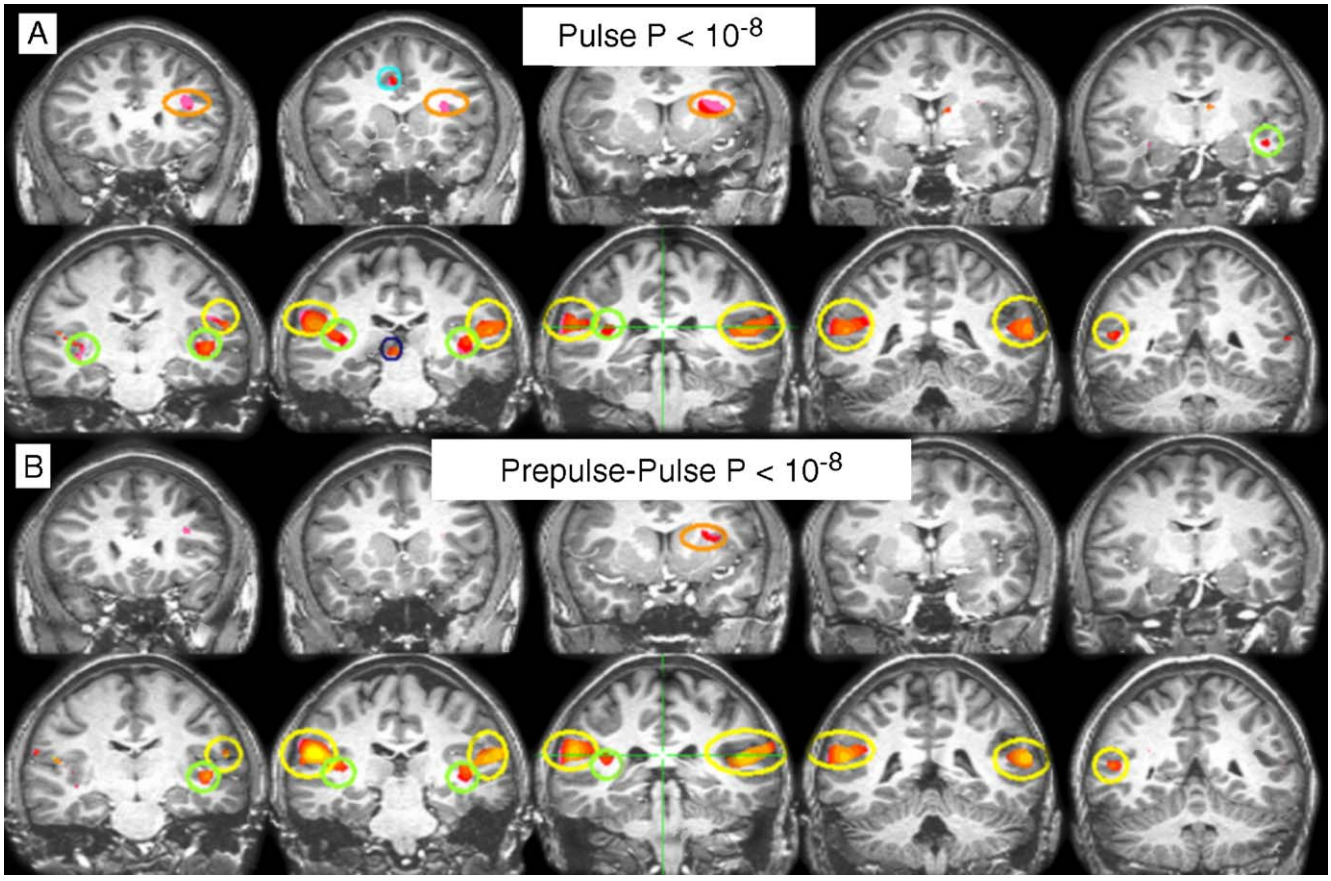

Fig. 1. Brain areas activated by pulse alone (A) and prepulse–pulse (B). Each panel shows the same ten (of twenty total) slices with overlaid BOLD responses in five contiguous voxels; each voxel significant at $P < 10^{-8}$. Underlying anatomic scan is from one of the subjects and is for illustrative purposes only. Circles identify areas of cortical and sub-cortical activity as follows: orange = dorsal striatum (L); light blue = anterior cingulate (R); yellow = 1°, 2° auditory cortices, supramarginal gyrus (R, L); green = insula (R, L); dark blue = midbrain (L). Activity in other slices was observed in the cerebellum, parahippocampal gyrus and thalamus at this level of significance.

coefficients for each trial type were then extracted for each active voxel. Data were then analyzed with a region-wise three-level repeated measures mixed-effects model (Laird and Ware, 1982), in which subject was the level three factor, voxel was the level two factor, while the Trial Type (1 = pulse, 0 = prepulse–pulse) and TR (1 to 7) were level one factors (SPSS 12.0, O'Connell and McCoach, 2004; Leyland, 2004). At level three and two, the intercept was entered as a random effect. TR was treated as a random repeated effect at level 1, and its covariance structure was modeled as heterogeneous first order autoregressive (AR(1)) in order to account for the higher correlation between adjacent TRs. This approach thus compares responses between Trial Types at the voxel level and yields a single statistical measure per ROI for each comparison of interest (Gibbons et al., 2004).

The hemodynamic response function within each ROI was modeled as a 4th order polynomial, thus Time from −3 to +3 (i.e., linear trend), Time^2 (quadratic trend), Time^3 (cubic trend) and Time^4 (4th order trend) along with their interactions with Trial Type were entered as fixed effects in the model (Leyland, 2004). To address the possibility of lateralized findings, Side (1 for left, 0 for right) and its associated interaction terms were also entered as fixed effects. In addition to the lateralized effects, we also report the 'Trial Type', 'Time by Trial Type', and 'Time^2 by Trial Type' effects as these are most likely to reflect interpretable differences in the overall amplitude of the HRF (Table 1). Time was centered at the 4th TR, thus reported effects such as Trial Type reflect differences in percent signal change near the peak of the response (i.e., 6 s) in most (but not all) ROIs (e.g., see auditory cortex in Fig. 3). Our primary focus was on the 'Time^2 by Trial Type interaction,' which reflects whether the amplitude of the initial rise and fall in the HRF differed between trial types (Gibbons et al., 2004). A separate analysis revealed no Gender effect or Gender by Trial Type interaction.

In order to assess whether the timing of the HRFs differed in the two trial types, the temporal center of activity (TCA) for each active *positive* voxel was calculated using the following formula: $\text{TCA} = [\sum((\text{hn} - \text{hmin})\ (n + 1)\ \text{TR})/(\sum(\text{hn} - \text{hmin})] - \text{TR}$, where n = sampling time point (zero to seven), hn is nth regression coefficient of the HRF in that voxel, hmin is minimum regression coefficients in that voxel, and TR is repetition time in s (i.e., 2) (Zhu et al., 2005). TCA determines the time point which divides the percent signal change (i.e., area under the curve) from baseline into halves and thus is likely to reflect differences in timing of the BOLD response. Differences between trial types were also analyzed with a three-level mixed-effects regression model with subject entered as a random effect at levels 3 and 2 (Table 2). Finally, to further explore the relationship between neural activity and PPI, we considered the correlation between the difference in mean percent signal change for the two trial types (prepulse–pulse

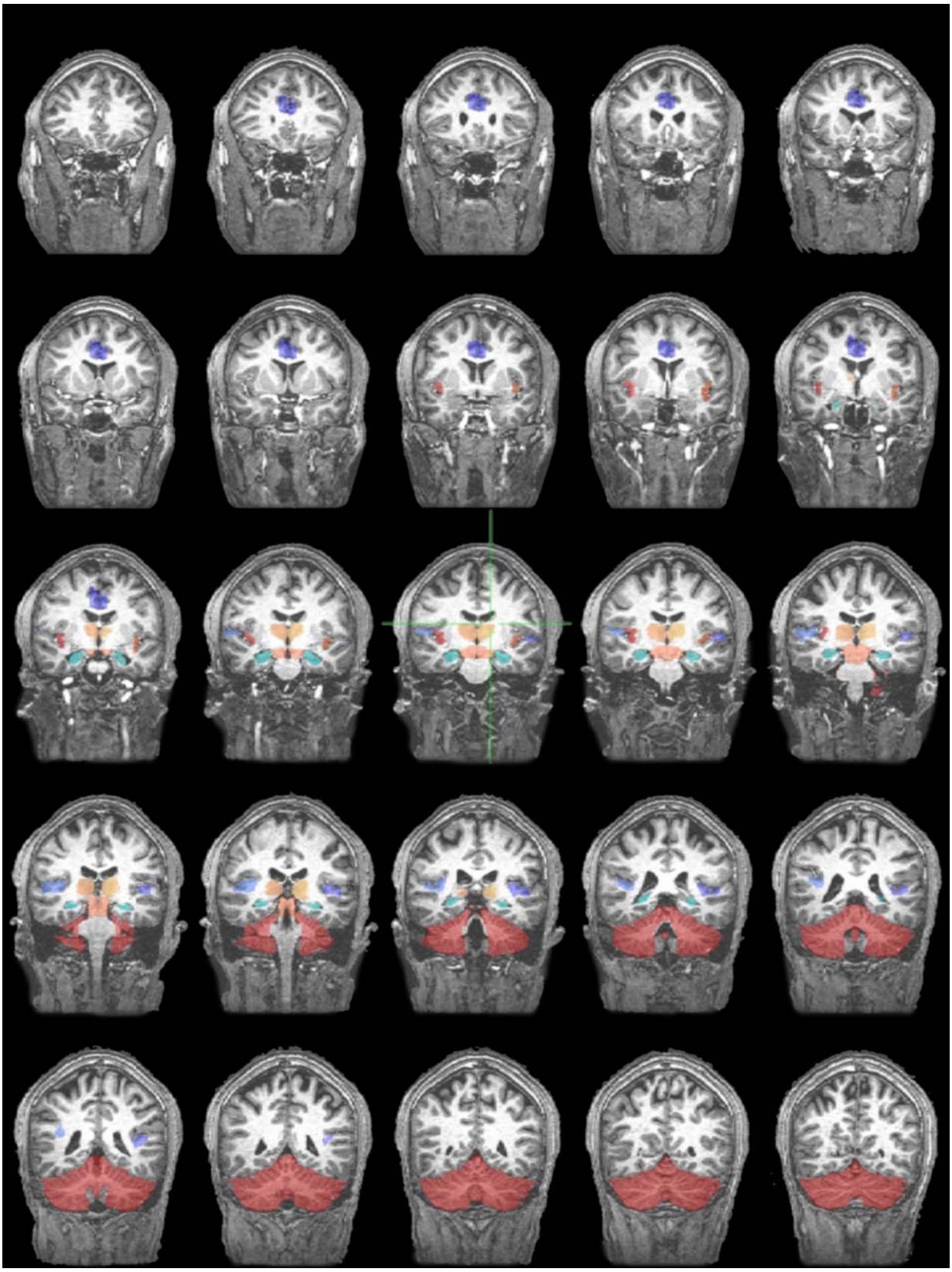

Fig. 2. Boundaries of regions of interest. Figure shows the manually traced ROI boundaries on all twenty five slices in one subject's images. ROIs were selected from areas of potential difference in the group analysis (i.e., Table 1) that showed activity at $P < 10^{-4}$ for at least 8 of the 14 subjects. Hippocampus was also included, even though it failed to meet the latter criteria. Colors denote brain structure as follows: hippocampus = green; primary and secondary auditory cortex = blue; insula = dark red; anterior cingulate = dark blue; pons–midbrain = pink; thalamus = orange; cerebellum = red.

Table 1
Tests of selected fixed effects from the hierarchical mixed-model regression of the hemodynamic response functions in each ROI[a]

ROI voxels[#]	Pons/Midbrain 16 ± 19 (0, 54)			Cerebellum 163 ± 205 (0, 667)			Thalamus 79 ± 78 (0, 205)			Auditory 88 ± 51 (1, 161)			Insula 41 ± 29 (1, 106)			Cingulate 41 ± 49 (0, 133)			Hippocampus 1.1 ± 1.4 (0, 5)		
	df	*F*	*P*[b]	*df*	*F*	*P*	*df*	*F*	*P*	*df*	*F*	*P*	*df*	*F*	*P*	*df*	*F*	*P*	*df*	*F*	*P*
Trial type	809	10.5	0.001	8432	113	0.001	4092	161	0.001	7250	7.1	0.008	2175	9.2	0.002	2106	61.6	0.001	35	0.67	0.418
Time by Type	1020	8.1	0.004	10,103	18.5	0.001	2319	7.6	0.006	3960	2010	0.001	3014	0.04	0.841	2820	7.1	0.008	57	0.09	0.762
Time^2 by Type	1006	1.8	0.178	8035	109	0.001	4196	60.7	0.001	6283	65.6	0.001	2091	17.8	0.001	2244	24	0.001	62	0.14	0.701
Side	–	–	–	2290	0.05	0.815	1659	11.4	0.001	9.95	5.4	0.041	606	0.29	0.590	597	6.8	0.009	11	0.18	0.673
Side by Type	–	–	–	12,550	8.2	0.004	3338	0.241	0.623	1485	0.8	0.358	3775	1.0	0.304	3829	0.328	0.567	66	1.0	0.312
Side by Time	–	–	–	5271	13.8	0.001	1826	0.024	0.878	3313	1026	0.001	1171	0.02	0.870	1504	28.7	0.001	38	0.01	0.906

[a] The hemodynamic response functions were modeled as 4th order polynomials and their interactions with trial type were entered as fixed effects in the model. To address the possibility of lateralized findings, side and its associated interaction terms were also entered as fixed effects. Time was centered at the 4th TR. Our primary focus was on the 'Time^2 by trial type interaction,' which reflects differences in the amplitude of the HRF. The trial type effect reflects differences in peak response if the peak occurs at 6 s. Higher order time terms and their interactions were highly significant ($P \ll .001$)in most cases but are omitted from the table as they are either difficult to interpret or of limited interest. See Methods for details.

[b] *P* values <0.001 are listed as 0.001.

[#] Values are mean ± SD of number of voxels meeting False Discovery Rate criteria for each subject in ROI. Range is in parentheses.

minus pulse) in each ROI with the subjects percent PPI obtained in the mock scanner.

Results

Simulated scanner

Mean ± SD percent prepulse inhibition (PPI) for all 41 subjects studied in the mock scanner was 11.7 ± 58.5%. For the 15 subjects selected to undergo fMRI scanning, mean PPI was 58.5 ± 22.2%.

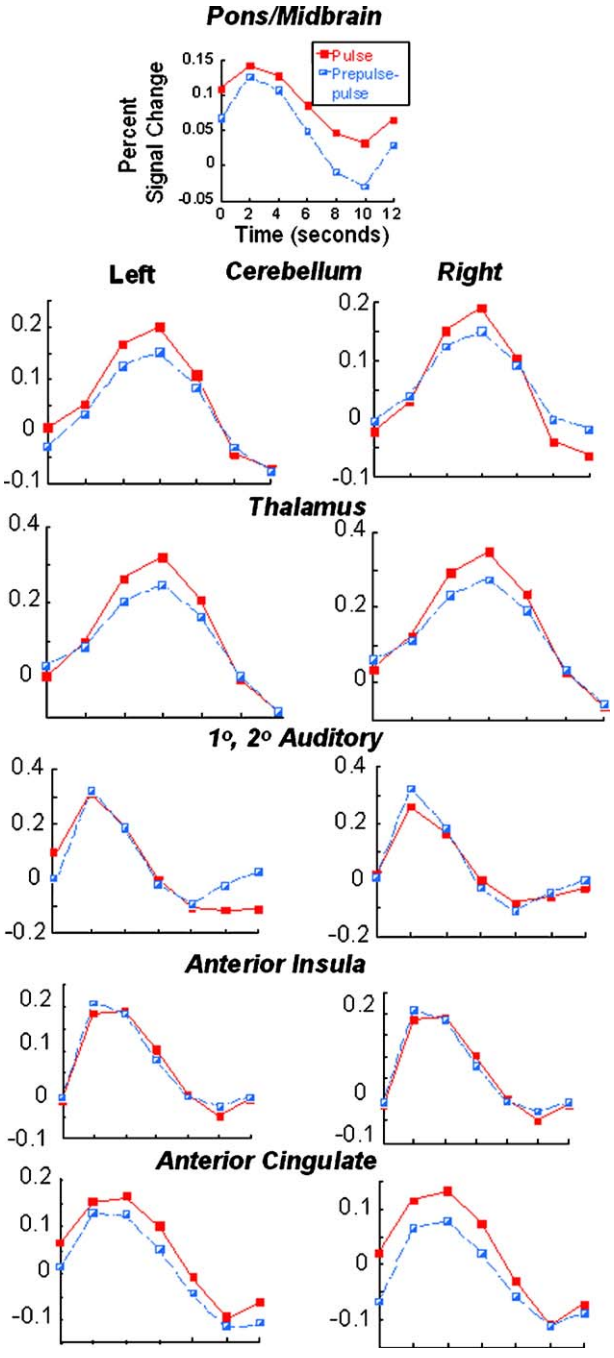

Fig. 3. Modeled hemodynamic response functions. Graphs show modeled HRFs for each trial type for each side.

Table 2
Temporal center of activity (mean ± SD) and fixed effects analyses in ROIs

ROI	Prepulse–pulse trials (seconds)	Pulse trials (seconds)	Fixed effects		
			Trial type	Side	Type × Side
			P value	*P* value	*P* value
Pons/Midbrain	5.66 ± 1.13	5.60 ± 1.48	0.34	–	–
Cerebellum	6.24 ± 1.13	5.99 ± 1.18	0.001	0.001	0.075
Thalamus	5.48 ± 1.31	5.73 ± 1.44	0.13	0.0003	0.57
Auditory Cortex	4.91 ± 1.02	4.72 ± 1.05	0.036	0.80	0.90
Insula	5.03 ± 1.19	4.88 ± 1.16	0.024	0.97	0.26
Cingulate	5.09 ± 1.07	4.99 ± 1.05	0.65	0.37	0.062
Hippocampus	6.81 ± 0.63	5.99 ± 0.78	0.29	0.77	0.58

fMRI results

One of the 15 scanned subjects was excluded from the analysis because of movement within runs that exceeded one voxel. All remaining participants (8 males, 6 females with mean ages of 23.2 ± 2.0 years) exhibited significant BOLD responses in primary auditory cortices. Motion between TRs did not differ significantly with $P > 0.2$ for those TRs that included pulse trials (0.184 ± 0.072 mm), prepulse–pulse trials (0.160 ± 0.064) or no trials (0.168 ± 0.082).

BOLD response to pulse alone and prepulse plus pulse trials

The analysis of thresholded volumes of activity revealed BOLD activity (3 or more voxels each with a *P* value $<10^{-8}$) following one or both trial types in the left midbrain, bilateral thalamus, cerebellum, bilateral primary/secondary auditory cortices extending into the supramarginal gyri, bilateral insulae, left dorsal striatum, right anterior cingulate and bilateral parahippocampal gyri (Fig. 1). While there were no areas where the responses to the two trial types differed significantly after correction for multiple comparisons with this approach, several areas showed subthreshold differences (five or more contiguous voxels each with a *P* value $<5.0 \times 10^{-3}$), suggesting that a more sensitive method might reveal differences in the underlying HRFs. These areas and their associated volumes included cerebellum (4.5 cm^3), right parahippocampal gyrus (1.2 cm^3), left anterior cingulate (1.0 cm^3), left parahippocampal gyrus (0.9 cm^3), right thalamus (0.7 cm^3), right hippocampus (0.6 cm^3), left hippocampus (0.4 cm^3), left precentral gyrus (0.4 cm^3), pons (0.2 cm^3), and right postcentral gyrus (0.2 cm^3).

Comparison of HRFs in regions of interest

Those areas noted above where at least eight subjects showed a significant BOLD response to the trials (i.e., uncorrected *P* value $<10^{-4}$) were then selected for further analysis (Fig. 2). Selected ROIs included the pons/midbrain, cerebellum, thalamus, primary/secondary auditory cortices, anterior insula, and anterior cingulate. In addition, despite activity in only three subjects, we examined the hippocampus due to its central role in sensory processing, prepulse inhibition and severe mental illness (Andreasen, 1999; Goldman and Mitchell, 2004; Tamminga and Holcomb, 2005) and the findings in previous fMRI studies (Kumari et al., 2003, Postma et al., 2006).

Fig. 3 shows the fitted models for the HRFs for each trial type in each ROI. Only the hippocampus failed to demonstrate a significant temporal response. In other ROIs, the linear, quadratic, cubic and fourth-order polynomials of the temporal response were almost all highly significant (i.e., *P* value $\ll 0.001$, Supplementary Table 1). Table 1 lists statistical findings of those effects most sensitive to differences in the amplitude of the trial types. Visual inspection and the statistical analysis in the pons indicated that percent signal change was consistently greater during pulse than prepulse–pulse trials (main effect Trial Type with a *P* value of 0.001) but that the overall magnitude of the change in the HRF and specifically the extent of the drop below baseline following the initial positive response (undershoot) were greater with prepulse–pulse trials (Time by Trial Type interaction *P* value of .004). In contrast to the pons, in other ROIs, values for the two trial types were generally similar both at the beginning and at the end of the HRF (Fig. 3). In the cerebellum, thalamus and anterior cingulate, the peak BOLD responses (Trial Type effect with *P* values <0.001) and overall rise and fall in BOLD activity (Time^2 by Trial Type interactions with *P* values <0.001) were diminished in the prepulse–pulse trials relative to the pulse trials. In contrast, amplitude in primary/secondary auditory cortices and the anterior insula was increased in the prepulse–pulse relative to pulse trials (i.e., Time^2 by Trial Type interactions with *P* values <0.001). The amplitudes differed on the two sides of the brain in many ROIs (significant Side or Side by Time effects in cerebellum, thalamus, auditory cortices and anterior cingulate, Supplementary Table 1), though only in the cerebellum was there a difference between the trial types (Side by Trial Type interaction with a *P* value of .004, Table 1, Fig. 3).

To compare the timing of the responses of each trial type, we calculated the temporal center of activity of the HRFs. This analysis revealed a relative delay for prepulse–pulse relative to pulse trials in the auditory cortices, anterior insula and cerebellum (Table 2). While there were lateralized differences in temporal center of activity in the cerebellum and thalamus, none of the differences varied by trial type (i.e., all Trial Type by Side with a *P* value >0.05). Percent PPI obtained outside of the scanner correlated significantly with the difference in the mean BOLD signal of the two trial types (prepulse–pulse minus pulse) in anterior insula ($r = 0.668$, $n = 14$, *P* value = 0.009) and cerebellum ($r = -0.724$, $n = 8$, *P* value = 0.024), but not with other regions.

Discussion

This is the first imaging study of prepulse inhibition using a rapid presentation event-related design. Our results show that BOLD activity associated with the prepulse inhibition of acoustic startle varies across several brain structures linked to both sensory integration and to neuropsychiatric disease. Thus, the amplitude of the hemodynamic response function (HRF) following prepulse–pulse trials was increased in the auditory cortices and anterior insula, while it was decreased in the cerebellum, thalamus and anterior cingulate compared to pulse alone trials (Fig. 3, Table 1). In the pons/midbrain, the amplitude was also decreased, though the extent of the signal change was actually greater due to a more extensive 'undershoot' of the HRF (Fig. 3). In addition to these differences in amplitude, the timing of the prepulse–pulse HRF was delayed in the cerebellum, auditory cortices and anterior insula. Finally, percent PPI was correlated with the greater

prepulse–pulse activity in the anterior insula and the diminished prepulse–pulse activity seen in the cerebellum. Previous studies link the pons, thalamus, secondary auditory cortices, anterior insula and anterior cingulate to sensory integration (Fendt et al., 2001; Swerdlow et al., 2001; Diederich and Koch, 2005; Pressler et al., 2005), while the thalamus, cerebellum, anterior insula and anterior cingulate are also linked to neuropsychiatric disorders (Andreasen et al., 1998; Pressler et al., 2005; Tamminga and Holcomb, 2005).

Consistent with others (Kumari et al., 2003; Postma et al., 2006), we found prepulse–pulse HRFs to be diminished in the cerebellum and enhanced in the insula relative to the pulse HRFs (Fig. 3, Table 1), whereas our findings of diminished prepulse–pulse HRFs in the thalamus and anterior cingulate conflict with previous reports (Hazlett et al., 2001; Kumari et al., 2003; Postma et al., 2006). In addition, we had selected our scanning parameters to optimize detection of HRFs in the hippocampus, hoping to reproduce others' findings. We were, however, unable to detect a clear signal with this ROI analysis. Perhaps louder acoustic pulses, which recent technological advances permit, or shortening the lead interval between prepulse and pulse to a more optimal 120 ms will enable signal detection in this region. Our group data, in contrast to our ROI analyses, were analyzed using methods similar to those of others and did identify significant activity associated with one or both trial types in many of the same areas others found activity (e.g., sensory motor cortices, supramarginal gyrus, hippocampus and striatum). Unlike others, however, we were unable to detect significant differences between trial types. These differences between studies may simply be attributable to differences in study design but could also reflect the diminished sensitivity of an event-related design or of acoustic stimuli.

Differences in BOLD activity across trial types, with the exception of those in the pons/midbrain, which may be confounded by brainstem artifacts (Komisaruk et al., 2002), are unlikely to be attributable to confounding factors because (a) we corrected for head motion and demonstrated that subject movement was not significantly increased with either trial type; (b) the event-related design should minimize extraneous activity that is captured with block designs; and (c) PPI in the mock scanner correlated with prepulse–pulse BOLD activity in the scanner, particularly in those regions thought to underlie sensory integration (i.e., anterior insula and cerebellum). It is important to consider, however, that other factors hinder interpretation of these data: (1) the inclusion of only subjects with the highest PPI (37% of total); (2) the increased number of trials (i.e., 200 total); (3) the loudness of the background; and (4) the confining scanner environment. Specifically, by studying only the subset of healthy controls with the highest PPI in the mock scanner, we cannot be certain that these findings are reflective of the general population nor does such a design promote comparisons between groups. Hence, future studies using this approach must either induce higher amounts of PPI (perhaps by further reducing the interference from scanner noise or by optimizing the timing between pulse and prepulse) or demonstrate that PPI is tightly linked to BOLD activity even in those subjects who do not show PPI in the scanner environment. Current evidence suggests that the other potentially confounding factors noted above may present less of an obstacle as percent PPI appears to be highly correlated within subjects despite the effects of trial repetition (Goldman et al., 2001; Quednow et al., 2006), background noise (Cadenhead et al., 1999; Flaten et al., 2005) or emotional state (Ludewig et al., 2002; Pijlman et al., 2003) (but see Grillon and Davis, 1997). Still, it will be important to definitively demonstrate that habituation associated with pulse intensity and subjective arousal in the scanner does not confound the findings. These issues can be addressed by utilizing concurrent measures of eye blink intensity (Kulkarni et al., 2004; Miller et al., 2005) and arousal (Williams et al., 2004).

The HRF differences between trial types are relatively subtle in that they were not apparent with an analysis based on the peak intensity in thresholded volumes but were highly significant following a polynomial modeling of the HRF. This approach to modeling the HRF with polynomials has not been utilized extensively with fMRI data (Gibbons et al., 2004); however, it would seem clearly indicated for situations, like this one, where one is employing event-related designs with very brief stimuli as well as similar trial types. The polynomials seemed to accurately model the underlying HRF as all four terms were highly significant in most ROIs. By providing a single statistical value for each regional contrast of interest, hierarchical models essentially eliminate the problem of accounting for multiple comparisons across voxels which plague other approaches. More experience is needed with this approach, however, to confirm that the correlation in activity across voxels is adequately addressed and that the quadratic polynomial sufficiently captures the amplitude of the HRF (Gibbons et al., 2004).

The findings also indicated a delay in the prepulse–pulse responses in the cerebellum, auditory cortex and anterior insula (Table 2). These findings cannot be attributed to the timing of the stimuli as pulse stimuli were 'lined up' so that the prepulse occurred first. Analogous timing differences in trial types have recently been noted in several brain regions with words versus nonwords and familiar versus novel faces (Henson et al., 2002). Furthermore, there is evidence that timing of responses may be shifted relative to normals in schizophrenia (Ford et al., 2005). While highly statistically significant, these timing differences were also subtle given the temporal resolution of fMRI (de Zwart et al., 2005). Thus, in addition to the caveat noted above for hierarchical models, the proposition that these differences reflect timing of neuroactivity rests on the assumptions that differences in timing are not due to neurovascular coupling (Henson et al., 2002). This issue may be better addressed in humans by using perfusion rather than BOLD contrast (Liu et al., 2005; van Gelderen et al., 2005) and can be directly examined in laboratory animals (Li and Yeomans, 2000).

These results compliment ongoing efforts to characterize early sensory processing in animal models and humans while facilitating efforts to identify putative defects associated with neuropsychiatric disease. The significance of the relative increases, decreases and delays in the prepulse–pulse HRFs is unclear at present, but the fact that differences between trial types varied across regions suggests that they are not simply due to diminished perception of the pulse (Swerdlow et al., 2005). In particular, the similarity (or possibly advance) in the timing of the prepulse–pulse HRF relative to the pulse HRF in the thalamus (Table 2), in association with the delays seen in areas associated with sensory integration (i.e., cerebellum, auditory cortices, anterior insula), and the significant positive correlation between PPI and prepulse–pulse BOLD activity in two of these regions (i.e., cerebellum, anterior insula) suggest that the thalamus may protect processing of the prepulse by delaying processing of the pulse (Blumenthal, 1999; Dawson et al., 2000; Fendt et al., 2001; Wynn et al., 2005). The processing of the pulse can be further explored by varying the delay between the

stimuli, while comparing the correlation between the intensity of thalamic activity and activity in these other regions across trial types (Solodkin et al., 2004). This in turn may enable investigators to begin to define the functional neurocircuitry associated with PPI in forebrain structures. Neural network models which will facilitate testing of these predictions are being developed (Schmajuk and Larrauri, 2005).

Acknowledgments

The authors would like to acknowledge the technical expertise and assistance of Robert Lyons, William Beith, Richard Mattioli and Douglas Ward; the advice and support of Drs., Leo Towle, Jeremy Skipper, Sarah Keedy, Roland Erwin, David Levin, Donald Hedeker, Robert Gibbons and Wen-Ming Luh; and the financial support of the Brain Research Foundation at the University of Chicago, and the National Alliance for Research in Schizophrenia and Affective Disorders for an Independent Investigator Award (MBG).

Appendix A. Supplementary data

Supplementary data associated with this article can be found, in the online version, at doi:10.1016/j.neuroimage.2006.04.228.

References

Andreasen, N.C., 1999. A unitary model of schizophrenia: Bleuler's "fragmented phrene" as schizencephaly. Arch. Gen. Psychiatry 56, 781–787.

Andreasen, N.C., Paradiso, S., O'Leary, D.S., 1998. "Cognitive dysmetria" as an integrative theory of schizophrenia: a dysfunction in cortical–subcortical–cerebellar circuitry? Schizophr. Bull. 24, 203–218.

Bleuler, E., 1911. Dementia Praecox or The Group of Schizophrenias, Translated by J. Zinkin (1950). International Univ. Press, Inc, New York.

Blumenthal, T.D., 1999. Short lead interval startle modification. In: Dawson, M.E., Schell, A.M., Bohmelt, A.H. (Eds.), Startle Modification. Cambridge University, Cambridge, UK, pp. 51–71.

Braff, D.L., Grillon, C., Geyer, M.A., 1992. Gating and habituation of the startle reflex in schizophrenic patients. Arch. Gen. Psychiatry 49, 206–215.

Braff, D.L., Geyer, M.A., Swerdlow, N.R., 2001. Human studies of prepulse inhibition of startle: normal subjects, patient groups, and pharmacological studies. Psychopharmacology (Berlin) 156, 234–258.

Burock, M.A., Buckner, R.L., Woldorff, M.G., Rosen, B.R., Dale, A.M., 1998. Randomized event-related experimental designs allow for extremely rapid presentation rates using functional MRI. NeuroReport 9, 3735–3739.

Cadenhead, K.S., Carasso, B.S., Swerdlow, N.R., Geyer, M.A., Braff, D.L., 1999. Prepulse inhibition and habituation of the startle response are stable neurobiological measures in a normal male population. Biol. Psychiatry 45, 360–364.

Cox, R., 1996. AFNI: software for analysis and visualization of functional magnetic resonance neuroimages. Comp. Biomed. Res. 29, 162–173.

Dawson, M.E., Schell, A.M., Hazlett, E.A., Nuechterlein, K.H., Filion, D.L., 2000. On the clinical and cognitive meaning of impaired sensorimotor gating in schizophrenia. Psychiatry Res. 96, 187–197.

de Zwart, J.A., Silva, A.C., van Gelderen, P., Kellman, P., Fukunaga, M., Chu, R., Koretsky, A.P., Frank, J.A., Duyn, J.H., 2005. Temporal dynamics of the BOLD fMRI impulse response. NeuroImage 24, 667–677.

Diederich, K., Koch, M., 2005. Role of the pedunculopontine tegmental nucleus in sensorimotor gating and reward-related behavior in rats. Psychopharmacology (Berlin) 179, 402–408.

Dimitrova, A., Weber, J., Maschke, M., Elles, H.G., Kolb, F.P., Forsting, M., Diener, H.C., Timmann, D., 2002. Eyeblink-related areas in human cerebellum as shown by fMRI. Hum. Brain Mapp. 17, 100–115.

Fendt, M., Li, L., Yeomans, J.S., 2001. Brain stem circuits mediating prepulse inhibition of the startle reflex. Psychopharmacology (Berlin) 156, 216–224.

Flaten, M.A., Nordmark, E., Elden, A., 2005. Effects of background noise on the human startle reflex and prepulse inhibition. Psychophysiology 42, 298–305.

Ford, J.M., Johnson, M.B., Whitfield, S.L., Faustman, W.O., Mathalon, D.H., 2005. Delayed hemodynamic responses in schizophrenia. NeuroImage 26, 922–931.

Forman, S.D., Cohen, J.D., Fitzgerald, M., Eddy, W.F., Mintun, M.A., Noll, D.C., 1995. Improved assessment of significant activation in functional magnetic resonance imaging (fMRI): use of a cluster-size threshold. Magn. Reson. Med. 33, 636–647.

Genovese, C.R., Lazar, N.A., Nichols, T., 2002. Thresholding of statistical maps in functional neuroimaging using the false discovery rate. NeuroImage 15, 870–878.

Geyer, M.A., McIlwain, K.L., Paylor, R., 2002. Mouse genetic models for prepulse inhibition: an early review. Mol. Psychiatry 7, 1039–1053.

Gibbons, R.D., Lazar, N.A., Bhaumik, D.K., Sclove, S.L., Chen, H.Y., Thulborn, K.R., Sweeney, J.A., Hur, K., Patterson, D., 2004. Estimation and classification of fMRI hemodynamic response patterns. NeuroImage 22, 804–814.

Goldman, M.B., Mitchell, C.P., 2004. What is the functional significance of the hippocampal pathology in schizophrenia? Schizophr. Bull. 30, 367–392.

Goldman, M.B., Shah, J., Levin, D., Small, S., Heidinger, L., Torres, I., 2001. Adaptation of prepulse inhibition to fMRI. Soc. Neurosci. 737, 16 (abstract).

Grillon, C., Davis, M., 1997. Effects of stress and shock anticipation on prepulse inhibition of the startle reflex. Psychophysiology 34, 511–517.

Hazlett, E.A., Buchsbaum, M.S., Haznedar, M.M., Singer, M.B., Germans, M.K., Schnur, D.B., Jimenez, E.A., Buchsbaum, B.R., Troyer, B.T., 1998. Prefrontal cortex glucose metabolism and startle eyeblink modification abnormalities in unmedicated schizophrenia patients. Psychophysiology 35, 186–198.

Hazlett, E.A., Buchsbaum, M.S., Tang, C.Y., Fleischman, M.B., Wei, T.C., Byne, W., Haznedar, M.M., 2001. Thalamic activation during an attention-to-prepulse startle modification paradigm: a functional MRI study. Biol. Psychiatry 50, 281–291.

Hemsley, D.R., 2005. The schizophrenic experience: taken out of context? Schizophr. Bull. 31, 43–53.

Henson, R.N., Price, C.J., Rugg, M.D., Turner, R., Friston, K.J., 2002. Detecting latency differences in event-related BOLD responses: application to words versus nonwords and initial versus repeated face presentations. NeuroImage 15, 83–97.

Kim, D., Adalsteinsson, E., Glover, G., Spielman, D., 2002. Regularized higher-order in vivo shimming. Magn. Reson. Med. 48, 715–722.

Komisaruk, B.R., Mosier, K.M., Liu, W.C., Criminale, C., Zaborszky, L., Whipple, B., Kalnin, A., 2002. Functional localization of brainstem and cervical spinal cord nuclei in humans with fMRI. Am. J. Neuroradiol. 23, 609–617.

Kulkarni, K., Heidinger, L., Goldman, M.B., 2004. Demonstrating prepulse inhibition of acoustic startle in normals during FMRI. Int. Soc. NeuroImaging Psychiatry 22 (abstract).

Kumari, V., Postma, P., 2005. Nicotine use in schizophrenia: the self medication hypotheses. Neurosci. Biobehav. Rev. 29, 1021–1034.

Kumari, V., Gray, J.A., Geyer, M.A., Ffytche, D., Soni, W., Mitterschiffthaler, M.T., Vythelingum, G.N., Simmons, A., Williams,

S.C., Sharma, T., 2003. Neural correlates of tactile prepulse inhibition: a functional MRI study in normal and schizophrenic subjects. Psychiatry Res. 122, 99–113.
Kumari, V., Antonova, E., Zachariah, E., Galea, A., Aasen, I., Ettinger, U., Mitterschiffthaler, M.T., Sharma, T., 2005. Structural brain correlates of prepulse inhibition of the acoustic startle response in healthy humans. NeuroImage 26, 1052–1058.
Laird, N.M., Ware, J.H., 1982. Random effects models for longitudinal data. Biometrics 38, 963–974.
Leyland, A.H., 2004. A review of multilevel modeling in SPSS. www.mlwin.com/softrev/reviewspss.pdf
Li, L., Yeomans, J.S., 2000. Using intracranial electrical stimulation to study the timing of prepulse inhibition of the startle reflex. Brain Res. Brain Res. Protoc. 5, 67–74.
Liu, H.L., Feng, C.M., Li, J., Su, F.C., Li, N., Glahn, D., Gao, J.H., 2005. Disparity of activation onset in sensory cortex from simultaneous auditory and visual stimulation: differences between perfusion and blood oxygenation level-dependent functional magnetic resonance imaging. J. Magn. Reson. Imaging 21, 111–117.
Ludewig, S., Ludewig, K., Geyer, M.A., Hell, D., Vollenweider, F.X., 2002. Prepulse inhibition deficits in patients with panic disorder. Depress. Anxiety 15, 55–60.
Maschke, M., Erichsen, M., Drepper, J., Jentzen, W., Muller, S.P., Kolb, F.P., Diener, H.C., Timmann, D., 2003. Cerebellar representation of the eyeblink response as revealed by PET. NeuroReport 14, 1371–1374.
Meincke, U., Light, G.A., Geyer, M.A., Braff, D.L., Gouzoulis-Mayfrank, E., 2004a. Sensitization and habituation of the acoustic startle reflex in patients with schizophrenia. Psychiatry Res. 126, 51–61.
Meincke, U., Morth, D., Voss, T., Thelen, B., Geyer, M.A., Gouzoulis-Mayfrank, E., 2004b. Prepulse inhibition of the acoustically evoked startle reflex in patients with an acute schizophrenic psychosis—A longitudinal study. Eur. Arch. Psychiatry Clin. Neurosci. 254, 415–421.
Miller, M.J., Li, L., Weiss, C., Disterhoft, J.F., Wyrwicz, A.M., 2005. A fiber optic-based system for behavioral eyeblink measurement in a MRI environment. J. Neurosci. Methods 141, 83–87.
Neter, J., Kutner, M.H., Nachtsheim,, Wasserman, W., 1996. Applied Linear Statistical Models, 4th ed. Irwin, Chicago.
O'Connell, A.A., McCoach, D.B., 2004. Applications of hierarchical linear models for evaluations of health interventions: demystifying the methods and interpretations of multilevel models. Eval. Health Prof. 27, 119–151.
Oldfield, R.C., 1971. The assessment and analysis of handedness: the Edinburgh inventory. Neuropsychologia 9, 97–113.
Pijlman, F.T., Herremans, A.H., van de Kieft, J., Kruse, C.G., van Ree, J.M., 2003. Behavioural changes after different stress paradigms: prepulse inhibition increased after physical, but not emotional stress. Eur. Neuropsychopharmacol. 13, 369–380.
Pissiota, A., Frans, O., Fredrikson, M., Langstrom, B., Flaten, M.A., 2002. The human startle reflex and pons activation: a regional cerebral blood flow study. Eur. J. Neurosci. 15, 395–398.
Postma, P., Gray, J.A., Sharma, T., Geyer, M., Mehrotra, R., Das, M., Zachariah, E., Hines, M., Williams, S.C., Kumari, V., 2006. A behavioural and functional neuroimaging investigation into the effects of nicotine on sensorimotor gating in healthy subjects and persons with schizophrenia. Psychopharmacology (Berlin) 184, 589–599.
Pressler, M., Nopoulos, P., Ho, B.C., Andreasen, N.C., 2005. Insular cortex abnormalities in schizophrenia: relationship to symptoms and typical neuroleptic exposure. Biol. Psychiatry 57, 394–398.
Quednow, B.B., Kuhn, K.U., Beckmann, K., Westheide, J., Maier, W., Wagner, M., 2006. Attenuation of the prepulse inhibition of the acoustic startle response within and between sessions. Biol. Psychol. 71, 256–263.
Rissling, A.J., Dawson, M.E., Schell, A.M., Nuechterlein, K.H., 2005. Effects of perceptual processing demands on startle eyeblink modification. Psychophysiology 42, 440–446.
Schmajuk, N.A., Larrauri, J.A., 2005. Neural network model of prepulse inhibition. Behav. Neurosci. 119, 1546–1562.
Solodkin, A., Hlustik, P., Chen, E.E., Small, S.L., 2004. Fine modulation in network activation during motor execution and motor imagery. Cereb. Cortex 14, 1246–1255.
Swerdlow, N.R., Geyer, M.A., Braff, D.L., 2001. Neural circuit regulation of prepulse inhibition of startle in the rat: current knowledge and future challenges. Psychopharmacology (Berlin) 156, 194–215.
Swerdlow, N.R., Stephany, N.L., Talledo, J., Light, G., Braff, D.L., Baeyens, D., Auerbach, P.P., 2005. Prepulse inhibition of perceived stimulus intensity: paradigm assessment. Biol. Psychol. 69, 133–147.
Tamminga, C.A., Holcomb, H.H., 2005. Phenotype of schizophrenia: a review and formulation. Mol. Psychiatry 10, 27–39.
Thorne, G.L., Dawson, M.E., Schell, A.M., 2005. Attention and prepulse inhibition: the effects of task-relevant, irrelevant, and no-task conditions. Int. J. Psychophysiol. 56, 121–128.
Van den Buuse, M., Garner, B., Koch, M., 2003. Neurodevelopmental animal models of schizophrenia: effects on prepulse inhibition. Curr. Mol. Med. 3, 459–471.
van Gelderen, P.W.H., Wu, C., de Zwart, J.A., Cohen, L., Hallett, M., Duyn, J.H., 2005. Resolution and reproducibility of BOLD and perfusion functional MRI at 3.0 Tesla. Magn. Reson. Med. 54, 569–576.
Ward, B., 2002. Deconvolution Analysis of fMRI Time Series Data. Biophysics Research Institute, Milwaukee, WI.
Weiss, I.C., Feldon, J., 2001. Environmental animal models for sensorimotor gating deficiencies in schizophrenia: a review. Psychopharmacology (Berlin) 156, 305–326.
Williams, L.M., Das, P., Harris, A.W., Liddell, B.B., Brammer, M.J., Olivieri, G., Skerrett, D., Phillips, M.L., David, A.S., Peduto, A., Gordon, E., 2004. Dysregulation of arousal and amygdala–prefrontal systems in paranoid schizophrenia. Am. J. Psychiatry 161, 480–489.
Wynn, J.K., Sergi, M.J., Dawson, M.E., Schell, A.M., Green, M.F., 2005. Sensorimotor gating, orienting and social perception in schizophrenia. Schizophr. Res. 73, 315–319.
Zhu, D.C., Heidinger, L., Kulkarni, K., McLaren, D.G., Goldman, M.B., 2005. Brain activation temporal characteristic mapping in event-related fMRI studies. The Organization for Human Brain Mapping, 11th Annual Meeting 2005, Toronto, #596.